

LIBRARY
ROYAL AIRCRAFT ESTABLISHMENT
BEDFORD.

R. & M. No. 3242



MINISTRY OF AVIATION

AERONAUTICAL RESEARCH COUNCIL
REPORTS AND MEMORANDA

The Test Performance of Highly Loaded Turbine Stages Designed for High Pressure Ratio

By I. H. JOHNSTON and D. C. DRANSFIELD

LONDON: HER MAJESTY'S STATIONERY OFFICE

1962

PRICE: 12s. 6d. NET

The Test Performance of Highly Loaded Turbine Stages Designed for High Pressure Ratio

By I. H. JOHNSTON and D. C. DRANSFIELD

COMMUNICATED BY THE DEPUTY CONTROLLER AIRCRAFT (RESEARCH AND DEVELOPMENT),
MINISTRY OF AVIATION

*Reports and Memoranda No. 3242**

June, 1959

Summary. A blade design for a highly loaded two-stage turbine is described and the test performance of the turbine is presented.

Some of the factors affecting the performance and matching of turbine blade rows operating at supersonic gas velocity are discussed and investigated by means of tests on a three-dimensional nozzle cascade tunnel and on a variety of single-stage turbine builds.

1.0. *Introduction.* The design of a turbine to produce economical shaft power from a small gas mass flow with a high available pressure ratio of between 20 and 30/1, raises certain problems which are not generally encountered in the field of gas turbine design.

Blade designs can be approximately classified by the stage loading of the blading, and in general for good efficiency this does not exceed a value of 3.5; where loading is defined as $2kp\Delta T/u^2$ and where ΔT is the stage temperature drop and u is the mean blade speed.

At the level of blade speed considered acceptable for high temperature conditions, such a design may have blade exit gas velocities (relative to the blades) which approach or even slightly exceed a Mach number of 1.0, but inlet velocities relative to the blades are always well below sonic. Such a turbine could be used for the high pressure ratio duty, but it would require a considerable number of stages, and a small mass flow would necessitate very small blade heights in the early part of the expansion. Thus the resultant turbine would be large, complex, and probably not as efficient as the conservative stage loading might suggest.

The number of stages, and hence overall size and weight, can be reduced for a given blade speed by designing for higher stage loading. An extreme example of such a design is the velocity compounded two-stage turbine with an overall loading of approximately 18. This turbine comprises a row of nozzle blades across which the full expansion ratio is achieved, followed by three rows of impulse blading, the second of which is an impulse stator row which reverses the exit swirl from the first stage. Such a design is commonly referred to as a Curtis stage and is found in large steam turbines where it forms the first stage in the expansion, but in this application the blade speeds and pressure ratios are considerably lower than those now envisaged.

* Previously issued as N.G.T.E. Report No. R.235—A.R.C. 21,245.

Experience in the field of subsonic turbine performance would suggest that such high loading must necessarily be accompanied by low efficiency, but at pressure ratios of 20 or 30/1, much of the flow relative to the blading is considerably in excess of sonic velocity, so that the estimation of performance from subsonic data could be somewhat unrealistic.

This Report describes the turbine side of a combined turbine and cascade investigation carried out at the National Gas Turbine Establishment with the object of determining the performance obtainable in such a velocity compounded turbine when operated at high pressure ratio.

It was decided to make use of an existing experimental turbine and, for a first attempt, to design the blading by interpreting steam turbine practice where applicable. The first section of this Report describes the design, instrumentation and testing of this turbine and the subsequent parts deal with the development test work on the rig, and the associated analysis. In parallel with the turbine work, the blade design problems have also been investigated in cascade. Where relevant, the results of the latter work are drawn upon in this Report.

2.0. *Two-Stage Tests of Original Blading.* 2.1. *General Design of Turbine and Test Rig.* The experimental turbine¹ which was used in this investigation was of a design permitting considerable flexibility in build and had provision for assembly with one, two or three stages. The two-stage version was selected and the aim of the redesign was to adapt the turbine for the high pressure ratio duty by utilizing as much of the existing turbine as possible while preserving those parts in their original state for future use.

The blade annulus of the resultant high pressure ratio build is shown in Fig. 1, the major modifications to the original turbine being associated with the nozzle row. As all the expansion was designed to take place across this row, a robust construction was required and the nozzle blades were retained by a root fixing at their outer diameter within a complete ring which was free to expand relative to the main turbine casing. The inner diameter nozzle shrouds were located on an inner drum which overlapped the rotor disc, incorporating a long labyrinth seal between the turbine annulus and the air space at the upstream face of the first rotor disc.

A sketch of the rig layout in the test cubicle is shown in Fig. 2. Inlet air to the turbine was supplied by a 10/1 pressure ratio compressor and passed through a control valve, an emergency trip valve, and a flow measuring section to the combustion chamber. Heated air then entered the turbine and after passing through the blade rows, was exhausted into a large duct which was maintained at sub-atmospheric pressure by an ejector driven by air from a 4/1 pressure ratio compressor. By this means turbine pressure ratios of up to 25/1 could be attained.

2.2. *Description of Blade Design.* 2.2.1. *Selection of design point.* The choice of design point conditions was influenced to a large extent by considerations of the air supplies which were available, and conditions finally selected are listed below.

Inlet pressure	132 lb/sq in. abs.
Inlet temperature	750 deg K
Mass flow	5 lb/sec
Total/static pressure ratio	22/1
Rotational speed (N)	10,000 rev/min

Simple analysis of velocity compounded blading suggests an optimum blade speed which corresponds to a u/c of 0.20, where u is the mean blade speed and c is the velocity equivalent of the isentropic temperature drop, and for this design the corresponding N/\sqrt{T} was 365.

2.2.2. *Velocity triangles.* For this velocity compounded design full expansion was assumed to take place across the nozzles with a loss represented by a velocity coefficient (i.e., $\frac{\text{actual discharge velocity}}{\text{isentropic discharge velocity}}$) of 0.95, the flow through the ensuing impulse blade rows being at constant static pressure and with losses represented by velocity coefficients of 0.91 for each blade row. These velocity coefficients were arbitrary values as no accurate data were available for the Mach number range under consideration.

Design values for flow angle and Mach number are listed below for each blade row.

	Angle (degrees) (measured from axial direction)	Mach number
Nozzle exit	74	2.39
First rotor inlet (relative)	69.85	1.90
First rotor exit (relative)	-69.85	1.63
Second stator inlet	62	1.20
Second stator outlet	-62	1.07
Second rotor inlet (relative)	44	0.70
Second rotor outlet (relative)	-56	0.627

Annulus heights which were designed to give (for the assumed losses) a constant static pressure at mean diameter through the turbine from nozzle exit to turbine exhaust are shown in Fig. 3.

2.2.3. *Nozzle blade design.* The design of the nozzle blades was essentially an exercise in passage design, the blades forming the walls of adjacent convergent-divergent passages.

In the design of the latter the following assumptions were made:

- (1) flow within passage is isentropic
- (2) coefficient of discharge is unity
- (3) the loss, represented by a velocity coefficient of 0.95 is concentrated at the trailing-edge plane
- (4) blade height is constant and equal to the annulus height downstream of the trailing edge.

To obtain the design outlet flow angle of 74 deg it was found necessary to lay out the passage centre-line exit angle at approximately 76 deg to satisfy continuity of flow under the assumed pressure loss condition.

A sketch of the nozzle blade form at mean diameter is given in Fig. 4. 19 blades were selected, this choice being influenced primarily by the desire to keep passage dimensions large, relative to manufacturing tolerances. In comparison with a larger number of small chord blades, there is a possible penalty due to increased friction loss, but it was felt that this might well be counterbalanced by the reduction in number of flow disturbances associated with each trailing edge. The passage was formed to provide all the required turning upstream of the throat, after which the passage diverged with an included angle of approximately 15 deg. The final straight part of the suction surface was made parallel to the centre-line of the passage as it was believed that by this means, the design area ratio for the nozzles and the flow direction at the plane of the trailing edge could best be defined.

The nozzles were formed with integral platforms and shrouds which met the blade form in a 5/32 in. radius fillet and, as shown in Fig. 4, this fillet was taken into account in the calculation of throat and passage areas. To minimize inter-shroud leakage, narrow slots were machined along adjacent faces of the shroud platforms to carry metal sealing strips, but subsequent turbine tests showed that this was not completely effective and leakage was only finally eliminated by welding the nozzles together along the top and bottom shrouds into a complete nozzle ring.

2.2.4. *Rotor blade design.* In some respects the rotor blades presented the more difficult design problem as little was known regarding the performance of high deflection blading operating in the 1.0 to 2.0 Mach number range. The blade form shown in Fig. 5 is of the conventional steam turbine impulse design with sharp leading and trailing edges and with, two-dimensionally, a constant passage width. The design represents a compromise arrived at in the light of several empirical rules derived from steam turbine practice. These are listed below for this blade row.

- (1) Upper surface at leading and trailing edges tangential to inlet and outlet design flow angles.
- (2) Zero curvature on upper surface between throat and trailing edge.
- (3) Radius of curvature of lower surface (R_1) matched to a standard cutter size (for ease of manufacture).
- (4) Mean radius of curvature of flow path not less than twice the throat width. (For any value of R_1 this defines a maximum pitch.)
- (5) Blade axial width not more than 1.00 in. (This condition imposed by existing turbine scantlings.)
- (6) Blade form untwisted and of constant section.

In an attempt to minimize losses, the trailing-edge thickness was limited to approximately 0.010 in., this representing the minimum value acceptable for manufacture.

The selected blade design may be summarized by the following parameters.

$$\begin{aligned} s/c &= 0.47 \\ w/R_m &= 0.331 \\ \beta_1 = -\beta_2 &= 69.85 \text{ deg} \end{aligned}$$

2.2.5. *Second-stage blading.* The second-stage stator blade is shown in Fig. 6 and the design method closely followed that detailed in the previous paragraph for the rotor blade design.

The second-stage rotor blade was the only blade in which design flow was subsonic. For this blade the exit angle was made larger than the inlet angle, the required impulse area ratio being obtained by an increase in flare. This made it possible to employ a more conventional blade form, as shown in Fig. 7, and the design was based on a T6 section² modified to give a straight-backed blade from throat to trailing edge.

2.3. *Instrumentation.* 2.3.1. *Pressure measurement.* The various positions for pressure measurement in the turbine annulus are shown in Fig. 1. At turbine inlet, two static tappings were connected to a calibrated Bourdon gauge, and this pressure was treated as inlet total pressure, the dynamic head in this region being negligible.

All other wall static pressures were measured on mercury manometers which could cover a range of both super- and sub-atmospheric pressures.

2.3.2. *Temperature measurement.* Gas temperatures at turbine inlet and exhaust were measured using chromel-alumel thermocouples housed in stagnation shields, the thermocouple responses being recorded on a potentiometer.

2.3.3. *Torque and speed.* Torque was transmitted to and measured by a Heenan and Froude dynamometer. Speed was registered on a Maxwell indicator coupled to the dynamometer and readings were checked at intervals against a Haslar tachometer and a tachronometer⁶.

2.3.4. *Air mass flow.* Air flow was measured by a British Standard's orifice installation, using a 3.00 in. diameter orifice in a pipe with a measured bore of 5.90 in. and D , $D/2$ tappings. As the orifice was situated downstream of the inlet valve, a wire mesh screen and honeycomb straightener were positioned 20 diameters upstream of the orifice, to smooth the flow and to eliminate swirl. As a further precaution all test running was made with the inlet valve in the fully open position, turbine pressure ratio being varied by ejector control.

2.4. *Test Results (Two-Stage).* Preliminary tests indicated a turbine static efficiency η_s of 58 per cent at the design conditions of 22/1 total/static pressure ratio and N/\sqrt{T} of 365. This was considerably below the nominal value of 70 per cent, which corresponded to the blading velocity coefficients assumed in the design, and no doubt the higher losses contributed to a mismatching of static pressure distribution which was observed by the inter-row static measurements. A further feature of the results was that the mass flow exceeded the design value by $6\frac{1}{2}$ per cent, and since nozzle throat areas were in good agreement with design values, it was deduced that some leakage path must exist which permitted flow to by-pass the nozzle throat. The source of the trouble was eventually traced to the inter-shroud gaps, and as mentioned in Section 2.2.3, this leakage was finally cured by welding the individual nozzle blades into a complete ring.

The mismatching referred to above is demonstrated in Fig. 9 which shows the axial distribution of measured static pressure compared with the design values estimated at outer diameter on a basis of constant mean diameter pressure.

It was observed that, over a range of turbine pressure ratio from 15/1 to 22/1, the pressures measured at nozzle and first rotor exit were virtually constant and this suggested a choking phenomenon associated with the second-stage stators. This appeared not improbable as at the design entry Mach number to this row of 1.20, the nominal permissible 'contraction' of flow area through the second-stage stator for starting is only 3 per cent.

A further modification was therefore introduced prior to retesting. For this the outer diameter flare was removed at the second-stage stators, as shown in Fig. 1, this providing an increased area for flow at the leading-edge plane.

Test results for this modified build are shown fully in Figs. 8, 9 and 10.

At design operating conditions, measured overall efficiency is $60\frac{1}{2}$ per cent and the curves of Fig. 8 (which show efficiency versus turbine velocity ratio, u/c) demonstrate the sensitivity of performance to changes in speed and pressure ratio.

$$\left[u/c \text{ is defined as } \left(\frac{\text{mean blade speed}}{\text{velocity equivalent of isentropic heat drop}} \right) \right]$$

Fig. 9 shows pressure distribution measured at a constant speed of $N/\sqrt{T} = 334$ for a range of turbine pressure ratio. In comparison with the pressures obtained in the original tests, there is a slight improvement in expansion over the first stage, but it is uncertain whether this is due either

to the reduction in flow consequent upon the removal of leakage past the first nozzles or to the increased flow area provided at the leading edge of the second-stage stators. Increasing the turbine pressure ratio above 17/1 has no appreciable effect on pressure ratio across the first stage.

The effect of speed on pressure distribution is shown in Fig. 10. First-stage expansion increases as speed is reduced, but at all speeds a marked discrepancy exists between measured and design values of static pressure. It should be noted however, that plotting in terms of pressure distributions tends to give an exaggerated impression of the discrepancy between test and design performance. For example, the pressure measured at inner diameter for an overall ratio of 21.4/1 is included in Fig. 9, and, using a simple arithmetic mean, gives an average maximum nozzle expansion ratio of 11/1 as opposed to a design value of 22/1. This large difference in expansion ratio corresponds to a proportionately smaller difference in isentropic velocity, (V/\sqrt{T}), namely 103.64 compared with 112.60. Thus the actual gas velocities are not as far removed from design as might appear at first sight from the pressure distributions.

Consideration of the results described above led to the following tentative conclusions.

- (1) The blade losses must exceed those assumed in the design, but whether this inefficiency is common to both stages is not known.
- (2) The static pressure distribution, and hence, in all probability, the velocity distribution, along the turbine is significantly different from that which formed the basis of the design.
- (3) The reasons for the above mismatching are not fully understood, but the small improvement in efficiency consequent upon eliminating leakage and increasing blade height at second stator leading edge suggests that further increase in second-stage area might increase expansion over the first stage.
- (4) The conditions within the first stage approximate to impulse conditions, but the maximum first-stage pressure ratio that can be achieved is only approximately 10/1 compared with the design value of 22/1.

(Note: For first-stage pressure ratio the value P_{IN}/p_{s3} is used where p_{s3} is the static pressure at the outer wall. This ignores the radial pressure gradient at rotor outlet, with the result that true mean diameter pressure ratio will always exceed the nominal value.)

As in this velocity compounded design, the first stage should produce approximately 75 per cent of the total work output, it seemed probable that the efficiency of this stage was likely to dominate the overall performance. It was therefore decided to test the first stage alone, to provide a measure of its efficiency and also to show whether approximate impulse conditions might be obtained up to design pressure ratio when free from any choking constriction presented by the second stage.

In view of the convergent-divergent shape of the nozzle row passages and the fact that in the two-stage turbine these were constrained to operate at half their design pressure ratio, it was anticipated that if single-stage operation permitted full expansion, then any associated decrease in loss and hence, increase in efficiency in this stage, might indicate the order of improvement to be obtained in a turbine with a redesigned second stage.

3.0. *Single-Stage Tests of Original Blade Design.* 3.1. *Modification for Single-Stage Test.* The modifications required for single-stage testing were relatively simple, the original second-stage blading being removed and suitably shaped pieces inserted to fill up the gaps left in the outer annulus

wall and rotor disc (see Fig. 15). In addition to the instrumentation which was already available, two simple traverse probes were fitted in the annulus at rotor outlet to provide measurement of static and total pressure at exit from the stage.

3.2. *Test Results.* Turbine performance was measured at various rotational speeds over a range of pressure ratio. For these tests the pressure ratio was defined as the ratio $\frac{\text{Inlet total pressure}}{\text{Outlet static pressure}} P_{IN}/p_{s3}$ where p_{s3} was measured at the outer wall of the turbine annulus immediately downstream of the rotor blade row. The flow in this region has both high velocity and high swirl so that the mean stream pressure will be somewhat less than the measured value, with the result that the mean pressure ratio will be greater and efficiency smaller than the nominal values based on p_{s3} . However, the effect on efficiency will be less than 1 per cent and so the simpler and more reliable wall measurement was used as a datum, in preference to the alternative of static probe measurements at mean diameter.

Curves of static efficiency against u/c for four rotational speeds are shown in Fig. 11, static efficiency η_s being defined as the ratio $\Delta T/\Delta T_s'$ where ΔT is the total temperature drop across the stage and $\Delta T_s'$ is the isentropic temperature drop equivalent to the pressure ratio P_{IN}/p_{s3} . Efficiency is seen to increase with rotational speed, the optimum at each speed occurring at a pressure ratio of approximately 12/1.

The variations of static pressure at nozzle exit with stage pressure ratio are plotted in Fig. 12 for N/\sqrt{T} of 334* and for zero speed, and it is clear that at a stage pressure ratio of 12/1 the nozzle expansion approaches a limiting value (this value being dependent on speed). At stage pressure ratios greater than 12/1, further expansion must be confined to the flow at exit from the rotor blade row, and the leaving kinetic energy must therefore become increasingly large as compared with the stage work. This explains the fall off in static efficiency at the higher stage pressure ratios.

During the performance testing of the turbine, radial traverses for total and static pressure were made at exit from the rotor blade row. Using this basis for the measurement of outlet total pressure, values of total head efficiency η_T were computed and these are shown plotted against u/c in Fig. 13. It can be seen that for the speed range investigated, the total head efficiency increases with increasing pressure ratio, the optimum pressure ratio corresponding approximately with the design value, namely 22/1.

3.3. *Discussion.* From Figs. 11 and 13 it can be seen that, at the design conditions of speed and pressure ratio ($u/c = 0.2$), the static efficiency is 50.5 per cent and the total head efficiency is approximately 61.0 per cent. A standard of comparison is afforded by consideration of the design performance computed for this stage, assuming true impulse conditions and the nominal velocity coefficients of 0.95 for the nozzle row and 0.91 for the rotor row. The performance corresponding to these assumptions is a static efficiency of 54.6 per cent and a total efficiency of 68.6 per cent. It is clear that the losses occurring in the rotor blades, and/or the nozzle row, must exceed those assumed in the design. Also the static pressure distributions plotted in Fig. 5 show that the flow conditions within the turbine are different from those aimed at in the design, the mean diameter nozzle pressure ratio being only 13.1/1 in comparison with the design value of 22/1. This condition could itself contribute to the low efficiency in so far as we might anticipate that the performance of convergent-divergent nozzles may deteriorate when such nozzles are constrained to operate below their design pressure ratio.

* N/\sqrt{T} of 334 corresponds to a running speed of 8,000 rev/min and pressures were plotted for this condition to avoid the necessity for interpolating to obtain values for the design N/\sqrt{T} of 365.

This information regarding first-stage performance makes possible a somewhat more detailed appraisal of the two-stage results of Section 2.4. The operating condition to which the first stage was constrained is superimposed on Fig. 13 and it is clear that some improvement in efficiency would be obtained if the second stage could be modified to increase first-stage pressure ratio. A brief analysis, detailed in Appendix I, shows that the two-stage efficiency should rise from 60.5 per cent to 63 per cent, provided the necessary modification to second-stage geometry does not adversely affect the second-stage efficiency. It should be noted that such a mode of operation would require a Mach number at entry to the second stage of 1.1 (*cf.* original design value of 1.2), whereas analysis of the test results of Section 2.4 indicated the limiting Mach number to be approximately 0.7. It would be unwise to predict that the simple provision of increased flow area, by increasing blade height in the second stage, would secure operation at the required Mach number, but this difficulty could be avoided in an application featuring contra-rotation. Contra-rotation of the two rotor rows eliminates the necessity for the second-stage stator row, so that both the loss and choking problem associated with the second-stage stators are eliminated. A considerable improvement over the measured efficiency (60.5 per cent) might then be anticipated with confidence,

A major difficulty in assessing the general significance of the above results was ignorance regarding the sensitivity of performance to blade design, particularly rotor blade geometry. It was therefore decided to extend the test programme on the single-stage build and this work forms the subject of the following section.

4.0. *Single-Stage Tests of Modified Rotor Blading.* 4.1. *Introduction.* In parallel with the turbine test work which has been described in the previous parts of this Report, an investigation by Stratford and Sansome was in progress to examine the problem of rotor blade design for supersonic flow.

Briefly, this work consisted of an initial cascade test of the original first-stage rotor blade sections, in which the flow was studied by the Schlieren method of flow visualization and pressure traversing, followed by a series of tests in which certain blade design parameters were varied. The flow within the blade passage of the original blading was found to exhibit a severe shock pattern induced by the focusing of a series of weak compression waves which were propagated from the concave wall at passage entry, and met to form a shock close to the convex wall. This shock induced a heavy separation on the convex surface which produced a band of low energy in the exit flow. The influence of both blade pitch and passage curvature were investigated experimentally in cascade and also theoretically, and this work culminated in the design of a blade profile which, in cascade, gave a relatively shock-free passage flow.

The theoretical arguments developed by Stratford, which formed the basis of this design, are briefly summarized as follows:

The problem may be considered as one of passage design where the inlet flow is supersonic and uniform at a Mach number M_0 (giving a Mach angle μ_0) and the local passage shape is defined in terms of width w and mean radius of curvature r_m .

Consideration of the passage shape and Mach line configuration in the inlet section suggests that a criterion of the form $w/r_{m1} \leq (1/2M_0^2) + (1/4M_0^4)$ will ensure that the leading-edge Mach wave will intersect the suction surface of the passage, thus reducing the possibility of focusing of this and subsequent compression waves within the passage.

The approximate length of passage required for the above intercept is given by $w \cot \mu_0$.

Expansion occurs along the suction surface of the channel up to the above point, but if the passage be continued with unchanged curvature, this pressure gradient will reverse and pressure will rise to the original value, this cycle being repeated along the passage. If, however, the local curvature is doubled after the inlet section, a free vortex flow, having uniform boundary pressure distribution may be established.

Thus the criterion for passage shape after the inlet transition length is given by $w/r_{m2} = 2 \times w/r_{m1}$.

For both the original and modified blade designs, the total pressure loss was measured at a variety of spanwise positions, and the modified blade, as set up in the simple cascade tunnel, was shown to have a velocity coefficient of 0.952 compared with 0.929 for the original design.

For both designs the starting, *i.e.*, the establishment of supersonic flow through the blading, was sensitive to very small changes in geometry, and further work confirmed that starting could be rendered much less critical by the provision of a step increase in passage height at blade inlet. This practice is common in steam turbine design where the additional blade height is referred to as 'lap'.

In the light of these cascade investigations, a test programme to investigate the effects of both lap and profile shape was carried out on the turbine.

4.2. *Blade Details.* For economy and minimum manufacturing requirement the lap tests were schemed around the new profile, whereby starting with maximum lap, the one set of blades could be progressively cropped to illustrate the significance of lap, the final spanwise configuration to be identical with that of the original design, to provide a direct comparison between the two profile shapes.

A drawing of this new profile is shown in Fig. 14 and the significant differences between this and the original (Fig. 5) are listed below.

- (1) Both concave and convex surfaces contain double instead of single curvature, *i.e.*, there is a rudimentary transition curve between the straight and curved portions of the profile.
- (2) Pitch/chord ratio is reduced from 0.47 to 0.415.
- (3) The blade passage is no longer of constant width but incorporates a contraction at mean diameter of approximately 8 per cent.

(*Note:* Contraction should reduce local Mach number in the mid-chord region of the flow passages and hence frictional pressure loss. Due to use of constant section blading the contraction is greatest at root and least at tip. This is not unreasonable as radial pressure gradients at nozzle outlet will contribute towards higher Mach numbers at the root than at the tip, and as the Mach number increases, the permissible degree of contraction should also increase.)

- (4) The leading-edge wedge angle is reduced from 20 deg to 10 deg.

The spanwise configurations are shown in Figs. 14 and 15. For the first test, build two, the blade was unflared and a tip diameter was selected to equal the outer diameter at exit from the second-stage stators. (This limit was accepted to obviate extensive modifications to the second-stage annulus wall.) For subsequent tests, the leading-edge tip diameter was progressively reduced, and in the final configuration, the blade height and flare of the original design was reproduced.

4.3. *Test Results.* For each rotor configuration the turbine was tested over a range of speed and pressure ratio. In every case, the general nature of the curves of efficiency against u/c and of pressure distribution were similar to those observed with the original blading. A realistic comparison between the various tests can, therefore, be obtained from consideration of single points as in the table below.

Build No.	1	2	3	4	5
Design point performance Pressure ratio = 22/1 $N/\sqrt{x} = 365$	Original design	New profile			
		Full tip lap (17 per cent)	Half lap (with flare)	Zero lap (large flare)	Original flare
η_S	50.5	52	52.5	52	50
η_T	61	62.5	65	66	63.5
Mean diameter nozzle pressure ratio . . .	12/1	15/1	14/1	12/1	12/1

It should be noted that the values computed for total head efficiency are necessarily less accurate than the η_s values as the assessment for outlet total pressure depended upon a traverse of a stream of somewhat indeterminate inner boundary. For this reason the accuracy is assessed at approximately ± 1 per cent compared with the η_s accuracy of $\pm \frac{1}{2}$ per cent.

It should also be observed that the measurement of outer wall static pressure at nozzle exit was made from tappings which, for the lap configurations were necessarily positioned in a recess relative to the nozzle exit. The apparent increase in nozzle pressure ratio may, therefore, partially result from a local expansion round the step in the wall which precedes the point of measurement.

4.4. *Discussion.* Considering first tests 1 and 5 which compare the two profiles within an identical annulus geometry, there is little change in performance. The increase in total head efficiency for test 5 does suggest that the rotor velocity coefficient for the second blade design is slightly higher than for the original blading, but in view of the accuracy limitation, the change must be regarded as marginal.

A more marked change in performance is shown by comparison of 4 and 5 which illustrates the effect of exit blade height. As the nozzle pressure ratio is constant for these two builds the higher static efficiency of test 4 indicates an increase in absolute outlet swirl (V_{w3}), and as trailing-edge blade height is higher in test 4 there must also be a relatively smaller exit axial velocity. Thus both the absolute gas exit swirl angle (α_3) and the relative gas exit angle (α_2) must be greater for 4 than for 5. This would appear reasonable as the original flare was designed for a much higher velocity coefficient than exists in the turbine blading. For continuity to be satisfied with increase in loss, there must be some expansion at the rotor trailing edge with a resultant reduction in relative outlet angle*.

* Tests 4 and 5 are analysed in more detail in Section 6.0.

For tests 2, 3 and 4 the exit blade height is constant and therefore exit Va is approximately constant. Although the static efficiency is insensitive to leading-edge blade height, there is a progressive improvement in total head efficiency as lap is reduced. This indicates that there is a progressive increase in exit velocity as lap is reduced, which must be accompanied by an increase in gas outlet angle. For this to be so, the lap at leading edge must cause additional loss through the blade row, which, as in the case of insufficient flare, results in a deviation due to expansion at rotor trailing edge. The measured nozzle expansion increases as the lap is enlarged, but the uniformity of static efficiency suggests that any tendency for nozzle loss coefficient to diminish as its pressure ratio increases to nearer the design value is counteracted by an increase in pressure losses associated with the step in the outer wall.

4.5. *Effects of Blade Fouling.* In the course of test 5 a mechanical fault in the turbine permitted oil from the inlet bearing to enter the gas stream at inlet to the rotor blade row. This fault was later cured and the results shown in Section 4.3 are from repeat tests with no oil leakage, but the earlier test provided interesting evidence of the effect of fouling on performance. The effects of progressive fouling on performance are illustrated in Fig. 16, where both static and total efficiencies are related to nozzle expansion ratio. All of the points shown correspond to turbine operation at design pressure ratio and a speed (N/\sqrt{T}) of 334. This condition gives a u/c of 0.18 compared with the design value of 0.20 and this is the reason for the 'clean' efficiency values being below those shown in the table. The photograph on Fig. 16 shows the appearance of the rotor blades after running, a heavy deposit on the convex surface being clearly visible.

5.0. *Nozzle Test.* The turbine results of the preceding sections demonstrate that in every configuration tested the expansion ratio attained over the nozzle blades was markedly below that for which the blades were designed.

It can be argued that such a result can be due to either (a) excessive loss in the nozzle blade row resulting in insufficient flow area being available at exit from the nozzles, or (b) the outlet gas flow being in some way constrained to leave the nozzles at a higher angle than the design value. In either case, the effective reduction in outlet flow area would limit expansion ratio to a value less than design. A nozzle cascade test was performed to provide information on blade velocity coefficient and on the relation between flow angle and expansion ratio.

5.1. *Apparatus.* A drawing of the nozzle cascade is shown in Fig. 17. It comprised four turbine nozzles which simulated a segment of the turbine annulus followed by an enclosed exhaust section which was laid out with a helical path. Static tapings and provision for traversing were situated close to the trailing-edge plane and the angular position of one wall of the exhaust section was variable. It was assumed that outlet flow angle in the measurement plane would be controlled by this wall alone as, the flow being supersonic, any compression or expansion waves emanating from the other wall would only affect flow some way downstream of the plane of measurement (see Ref. 3).

5.2. *Results.* The performance of the nozzle row was measured over a range of wall outlet angle and for each angle the velocity coefficient based on an area mean of traverse total pressure was calculated. The variations of nozzle pressure ratio and velocity coefficient against wall angle are shown in Fig. 18, and whereas the maximum attainable pressure ratio is highly sensitive to wall angle, the velocity coefficient is effectively constant. Also shown are two calculated variations of pressure ratio with flow angle.

In the first of these the flow angles were calculated by using the average outlet total pressure and solving for continuity of flow on the basis of a uniform outlet distribution. This indicated a flow angle relative to the circumferential direction some 2 to 3 deg less than the measured wall angle.

The traverses had, however, indicated considerable non-uniformity of outlet total pressure and to determine the significance of this, a second estimate was made.

For this an extreme maldistribution was assumed in which a certain proportion of the outlet flow was taken to have a total pressure equal to the inlet total pressure, and the remainder to have a total pressure equal to the outlet static pressure. Using such a pressure distribution and adjusting the flow proportions so as to give a mean velocity coefficient equal to the measured value, the flow angle was again estimated and, as shown in Fig. 18, the calculated angle was now between $1\frac{1}{2}$ and 2 deg greater than the measured angle.

On the basis of these extreme comparisons the test figures may be regarded with reasonable confidence, and the results indicate that some account should be taken of maldistribution when designing such a nozzle row. For example, for the blade row tested, to produce the effective pressure ratio/flow angle relationship, it would be necessary to calculate exit flow area on the basis of uniform distribution and a velocity coefficient of 0.955 and then to use an empirical area correction X of approximately 1.15 where area correction is defined as

$$X = \frac{\text{true area required}}{\text{flow area based on uniform pressure}}$$

In comparison with the above result, a two-dimensional cascade test³ gave a velocity coefficient of 0.98, so that more than half the effective loss in the turbine nozzles must be associated with secondary flows induced by the annulus curvature.

It may be argued that some improvement in both pressure loss and flow distribution might result from a redesign of the nozzle blade row to incorporate a larger number of small chord blades. Such a configuration would present a reduced end-wall area to the gas flow and the consequent reductions in boundary layer might substantially reduce the associated secondary flows. The large blade chord of the experimental turbine was selected (*see* Section 2.2.3) to ensure that passage dimensions were large relative to the tolerances associated with an assembly of separate nozzle blades. It should be possible with a cast or welded nozzle ring to reduce the blade chord substantially while maintaining adequate control over individual passage dimensions, and indeed the leakage trouble experienced with separate blades suggests that such methods of construction are to be preferred.

6.0. *Analysis of Rotor Blade Performance.* The results of tests 4 and 5 are selected for analysis to investigate the effect of flare on blade performance.

The method adopted is to use the nozzle test results to provide values for flow angle and loss for the nozzle expansion measured in the turbine. For a given stage pressure ratio and static efficiency, one can compute the mean rotor exit conditions which will both correspond to the measured stage work output and also satisfy continuity of flow. A value of total head efficiency, related to the known static efficiency, may then be calculated. By this means it is possible to establish those nozzle and rotor flow conditions which most closely match the overall test measurements and the results of this assessment are set out in the following table.

Stage conditions: $P_{IN}/p_{s3} = 22/1$, $N/\sqrt{T_1} = 365$

Rotor flare	Test 4	Test 5	Design
η_S test per cent	52	50	} 54.6
η_S calculated per cent	52.5	51	
η_T test per cent	66	63	} 68.6
η_T calculated per cent	64.5	62.5	
ψ_R	0.872	0.844	0.91
α_1	74.5	74.5	70
α_2	69.4	65.5	70
M_0	2.13	2.13	2.39
M_1	1.61	1.61	1.90
M_2	1.64	1.56	1.63
M_3	1.20	1.17	1.20

The calculated values listed above are dependent upon the exit flow angle deduced from pressure measurements and the nozzle cascade tests of Section 5.2, but since the nozzle pressure ratio was identical for each test, the relative changes in rotor performance between tests 4 and 5 may be considered to be valid despite any doubts regarding the interpretation of nozzle cascade results.

It is apparent that the improvement in efficiency obtained with an increase in flare is accompanied by an increase in α_2 . This may be explained as follows:

With the smaller flare there is insufficient flow area in the passage for flow to achieve complete expansion and the full stage pressure ratio may then only be attained by a further free expansion with attendant pressure loss around the rotor trailing edge, the relative flow angle at rotor exit then being less than design. As flare is increased the larger exit flow area permits full expansion within the blade passage, flow angle approaches the design value, and the blade velocity coefficient rises from 0.844 to 0.872.

Although the deduced outlet angle for test 4 is in good agreement with the blade outlet angle, the velocity coefficient is still lower than that measured in cascade⁴. It would therefore appear that, as for the nozzle cascade, the radial pressure gradients found in the turbine promote secondary flows and losses which are not present in the two-dimensional cascade.

The loss data from the turbine tests are necessarily restricted to a particular configuration. In an attempt to provide a broader basis for performance analysis the generalized method for subsonic blading⁵ was applied to the supersonic blade. This assessment gives a rotor pressure loss coefficient (*i.e.*, ratio of total pressure loss to outlet relative dynamic head) of 0.724, which at the operating exit Mach number of 1.61 corresponds to a velocity coefficient of 0.91. It is not surprising that this value, associated with subsonic flow, should be higher than that deduced for the turbine, in which the rotor is undoubtedly subject to additional shock losses for which this method of assessment makes no allowance.

7.0. *Rotor Incidence.* The discrepancy between the design value of nozzle pressure ratio and the smaller maximum value actually achieved in the turbine was investigated by Stratford. His conclusions regarding the blade and nozzle interaction in supersonic flow were that the rotor/nozzle interaction may be considered as a shock phenomenon whereby the nozzles are constrained always

to deliver a supersonic flow at a unique incidence angle on to the following blade row, the angle being dependent upon rotor blade shape and Mach number. This incidence angle would be zero if the leading-edge thickness of the blades was zero, but becomes increasingly positive as blade leading-edge thickness increases.

This effect may be studied in the turbine by examining the results of test 5.

The maximum measured nozzle pressure ratio for a stage pressure ratio of 22/1 is plotted against rotational speed in Fig. 19A, and using the test relationship between flow angle and pressure ratio in the nozzle which has been described in Section 5.0 the inlet flow angles to the rotor blade were calculated. These values are compared in Fig. 19B with values of flow angle predicted by theory, taking into consideration the blade leading-edge thickness. Tolerable agreement is found for all but the design speed. The latter condition is that for which the blade inlet Mach number is a minimum, and the lack of agreement may be associated with shock losses which are ignored in the calculation. Such losses are most likely to be present at the higher rotational speeds, where the correspondingly lower inlet flow Mach number relative to the rotor blades increases the possibility of detached shock waves existing at the rotor leading edges.

To examine further the effect of rotor leading edge geometry the original blade design was modified as shown in Fig. 5 to provide a profile of negligible leading-edge thickness. Initial running at full pressure ratio and a speed of 8,000 rev/min ($N/\sqrt{T} = 334$) indicated an increase in nozzle pressure ratio from 13/1 to 16/1 and an improvement of between 0.5 to 1.0 per cent in efficiency. However as testing continued, the performance gradually fell off until it stabilized eventually at the same nozzle pressure ratio and efficiency as that for the unmodified blades.

Inspection of the blading showed that no serious fouling such as is described in Section 4.5 had occurred, the blades carrying only a thin carbon deposit which has been common to all the tests. The results suggest that refinement of the blade leading edge may have rendered it more susceptible to fouling.

Analysis of the initial 'clean' result on the basis of the nozzle tests (Section 5.0) indicates that the rotor blades were operating with a relative inlet gas angle of 71.8 deg. Although this is still higher than the nominal inlet angle of 70 deg, the change in relative inlet angle from approximately 74 deg (*see* Fig. 18B) for the unmodified leading-edge provides some further evidence to support the theory of leading-edge thickness effect.

It might be argued that in view of the slight effects on performance associated with this incidence effect it could be ignored in design, but it should be remembered that for the blades tested, the leading-edge thickness was smaller than might be attained in normal manufacture, particularly if the scale of the turbine is reduced.

In such a case, where leading-edge thickness, and hence incidence effect is large, there are two alternatives open to the designer.

- (1) If a symmetrical rotor blade form is preferred, the incidence effect will demand a smaller nozzle exit Mach number, and larger nozzle exit angle than indicated by simple impulse velocity triangles (*i.e.*, the design will be such as to give a small degree of reaction across the rotor row).
- (2) For a design where the nozzle area ratio matches the overall turbine pressure ratio, the rotor blades should incorporate a convergent passage, the blade leading edges being set to provide the requisite incidence to compensate for the leading-edge thickness. The gas

conditions will then be such that full turbine expansion takes place across the nozzle row, with a further expansion into the blade inlet, the convergent passage providing recompression through the rotor up to the required design pressure at exit.

Potentially, the second approach is likely to provide the greater work capacity for given rotor exit angle, blade speed and pressure ratio, but this may well be counterbalanced by increased rotor losses, and therefore the first approach with its simpler blade form is probably the more practicable.

8.0. *Partial Admission.* The final tests carried out on the high pressure ratio turbine were directed towards the effect of partial admission. Ten of the nineteen nozzle passages were blanked off leaving an admission of 47.4 per cent, and turbine efficiency was measured for both the single-stage and two-stage builds.

For both single and two-stage operation this degree of partial admission was found to cause a drop of two points in efficiency. This compares with a value of half a point in efficiency deduced for the single-stage build by the method of Ref. 7. Unfortunately, limitations of the test rig precluded the extension of this investigation to lower values of admission.

During the single-stage tests the static pressure upstream of the rotor was measured in the jet stream and in the no-flow region. It was noted that although the latter was equal to the turbine exit pressure, the pressure in the active jet remained close to the level measured in the full admission tests (Fig. 12). This suggests that the nozzle/rotor interaction previously observed with full admission (Section 7.0) is not significantly affected by partial admission.

9.0. *Comments and Conclusions.* Although the work described in this Report covers only a few of the many variables involved in a Curtis stage designed for high pressure ratio, the broad conclusion would seem to be that only small improvements over the original efficiency of 60.5 per cent are likely to be attained. To the reader who is conversant with gas turbine design, this figure may appear to be disastrously low, but the result appears in a more favourable light when one considers the implications of a conventional approach to the somewhat extreme design conditions.

If, for the same conditions of pressure ratio, blade speed and flow, we were to base the design on a stage loading ($2kp\Delta T/u^2$) of 3.5, the equivalent turbine requires six stages, on the assumption that for conventional scantlings, such a stage loading should lead to an efficiency of at least 85 per cent. In such a design the flow would be basically subsonic, and with an efficiency of 85 per cent compared with the Curtis efficiency of 60.5 per cent, there is an apparent economy of 29 per cent in flow for the same power output. When, however, we consider the scantlings for such a design to meet both the blade speed and rev/min conditions of the Curtis wheel, we find that first-stage blade height is only approximately 0.12 in., compared with 0.8 in. for the Curtis design.

Now the tip clearance used in the Curtis stage that has been tested was about 0.030 in., which is not excessive for a mean diameter of 14 in.; for the same tip clearance, but a blade height of 0.12 in., we could anticipate a substantial reduction in first-stage efficiency of possibly as much as 25 to 30 per cent. With higher blade heights in the subsequent stages this effect may be progressively reduced through the turbine, but it is not unreasonable to assume that the real efficiency would be more likely to be nearer 70 per cent than the original assumption of 85 per cent. In this case the real improvement in flow consumption would be only of the order of 14 per cent. If the blade chords were then reduced to give the same overall turbine size, there is likely to be a further penalty in performance due to the reduction in Reynolds number, so that for comparable weight there may be little improvement in consumption at the expense of considerable complexity in construction.

Although this tip clearance influence might be moderated by designing for higher rotational speed and hence lower diameter, any advantage gained by this approach might be counterbalanced by the additional requirement for a gear-box to provide shaft power at the design rev/min of the Curtis turbine.

Indeed, where consumption is not of prime importance but simplicity and light weight are at a premium, the best solution may be to use a single impulse stage which we have shown can provide an efficiency of approximately 52 per cent at the selected operating speed and pressure ratio.

The more detailed conclusions are listed below.

- (1) A two-stage turbine has been designed and tested over a range of pressure ratio and speed. At the design condition of pressure ratio = 22/1 and $N/\sqrt{T} = 365$, the measured static efficiency was 60.5 per cent.
- (2) The first stage of the above turbine when tested alone, gave, at the same conditions, a static efficiency of 50.5 per cent.
- (3) The flow conditions within the blading differed from those intended in the design due to choking within the second-stage stators, aggravated by the too optimistic loss assumptions made in the design calculations.
- (4) Elimination of second-stage stator choking should improve the performance of the two-stage build but, in view of the low supersonic Mach numbers at this point in the expansion, we cannot confidently predict that increased blade height would necessarily provide a complete solution. The best approach (if practicable) would be to use contra-rotation, which permits elimination of the offending blade row.
- (5) An alternative rotor blade design, shown to give improved performance in a simple cascade tunnel, provided little or no improvement in turbine efficiency.
- (6) Both nozzle and rotor blades gave substantially greater losses in the turbine than those measured in a cascade tunnel (inclusive of end losses). It is presumed that this is due largely to radial pressure gradients and associated flow deviations within the turbine stage.
- (7) The introduction of lap in the first stage improved the matching between stator and rotor flow conditions, but best single-stage performance was obtained with no lap and with a flare commensurate with the true blade losses. This enabled the flow to complete the expansion without deviation at rotor exit.
- (8) An interaction between the nozzle flow and the flow approaching the rotor blades has been demonstrated, which prevented full design expansion in the nozzles being achieved. The implications of this effect upon blade design have been discussed.
- (9) Both single-stage and two-stage turbine builds suffered a loss of two points in efficiency when operating with an admission of 47.4 per cent.

Acknowledgements. The authors are indebted to Mr. N. E. Waldren for his assistance with the mechanical design work associated with the investigation, to Mr. C. Hart who carried out the nozzle cascade work, to Mr. G. E. Sansome for assistance in operation of the test rig, and to Miss J. Marshall who was responsible for the computation of the results.

NOTATION

C	Blade chord
c	Velocity equivalent of isentropic heat drop
kp	Specific heat at constant pressure (ft pdl/lb/deg C)
N	Rotational speed (rev/min)
P_{IN}	Total pressure at turbine inlet
p_{s2}	Static pressure at exit from first nozzles
p_{s3}	Static pressure at exit from first stage
p_{s4}	Static pressure at exit from second-stage stators
p_{s5}	Static pressure at exit from second stage
p_N	Static pressure at nozzle exit (outer wall)
p_L	Static pressure at nozzle exit (inner wall)
R_M	Mean radius of rotor blade passage
S	Blade pitch
T	Gas temperature
ΔT	Turbine temperature drop
u	Mean blade speed
w	Width of rotor blade passage
X	Area coefficient for design of nozzle blades
α_0	Nozzle exit flow angle
α_1	Relative flow angle at rotor entry
α_2	Relative flow angle at rotor exit
α_3	Absolute flow exit angle
β_1	Rotor blade inlet angle
β_2	Rotor blade outlet angle
η_s	Turbine efficiency based on inlet total/outlet static pressure ratio
η_T	Turbine efficiency based on inlet total/outlet total pressure ratio
ψ_N	Nozzle velocity coefficient
ψ_R	Rotor velocity coefficient
M_0	Mach number at the passage entry
μ_0	Mach angle corresponding to M_0
r_{m1}	Radius of curvature of the passage centre-line at inlet
r_{m2}	Radius of curvature of the passage centre-line after inlet section

REFERENCES

<i>No.</i>	<i>Author</i>	<i>Title, etc.</i>
1	I. H. Johnston and G. E. Sansome	Tests on an experimental three-stage turbine fitted with low reaction blading of unconventional form. A.R.C. R. & M. 3220. January, 1958.
2	D. G. Ainley	The performance of axial-flow turbines. <i>Proc. Instn. Mech. Engrs.</i> 1948. Vol. 159.
3	B. S. Stratford and G. E. Sansome..	The performance of supersonic turbine nozzles. A.R.C. 21,261. June, 1959.
4	B. S. Stratford and G. E. Sansome..	Cascade tests on rotor blades for supersonic turbines. Unpublished M.O.A. Report.
5	D. G. Ainley and G. C. R. Mathieson	A method of performance estimation of axial-flow turbines. A.R.C. R. & M. 2974. December, 1951.
6	H. Shaw and W. E. Wilcox ..	The development of an accurate speed measuring device (the tachronometer). Unpublished M.O.A. Report.
7	Alan H. Stenning	Design of turbines for high-energy-fuel low-power-output applications. M.I.T. Dynamic analysis and Control Laboratory. Report No. 79. September, 1953.

APPENDIX I

The effect on performance of an increase in expansion over the first stage
(Based on original design blading)

From two-stage tests:

At P_{IN}/p_{s5} of 22/1, $\eta_s = 60.5$ per cent
but first-stage pressure ratio P_{IN}/p_{s3} is only 10/1.

From one-stage tests:

At $P_{IN}/p_{s3} = 10/1$, $\eta_s = 53.0$ per cent
 $\eta_T = 57.0$ per cent
 \therefore stage total pressure ratio = 7.9/1

hence overall pressure ratio for second stage is 2.79/1.

Knowing the performance for both one- and two-stage builds, it can be shown that the second-stage efficiency is 53.5 per cent.

If first-stage P_{IN}/p_{s3} is increased to 22/1, $\eta_s = 50.5$ per cent
 $\eta_T = 61.0$ per cent
 \therefore stage total pressure ratio = 10.3/1

and as a result, second-stage pressure ratio falls to 2.14/1.

If second-stage efficiency is assumed unchanged at 53.5 per cent, the new overall performance for the two stages may be computed to give an overall efficiency of 63 per cent.

Assumption $\gamma/(\gamma - 1) = 3.57$.

Note: Overall efficiency exceeds stage efficiencies due to the reheating effect of first-stage losses on second stage.

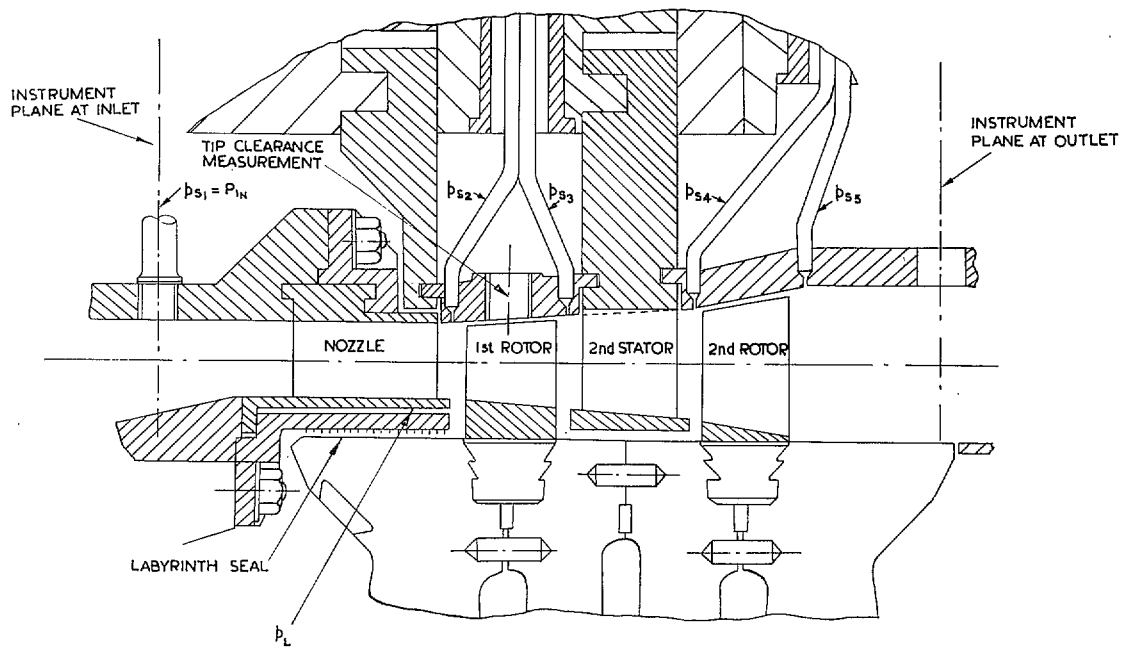


FIG. 1. Section of turbine annulus.

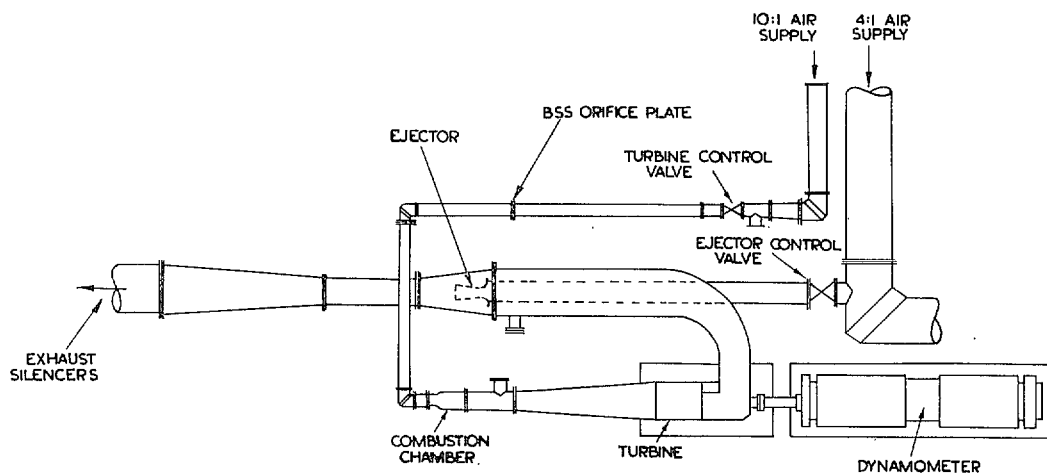


FIG. 2. Schematic layout of turbine test rig.

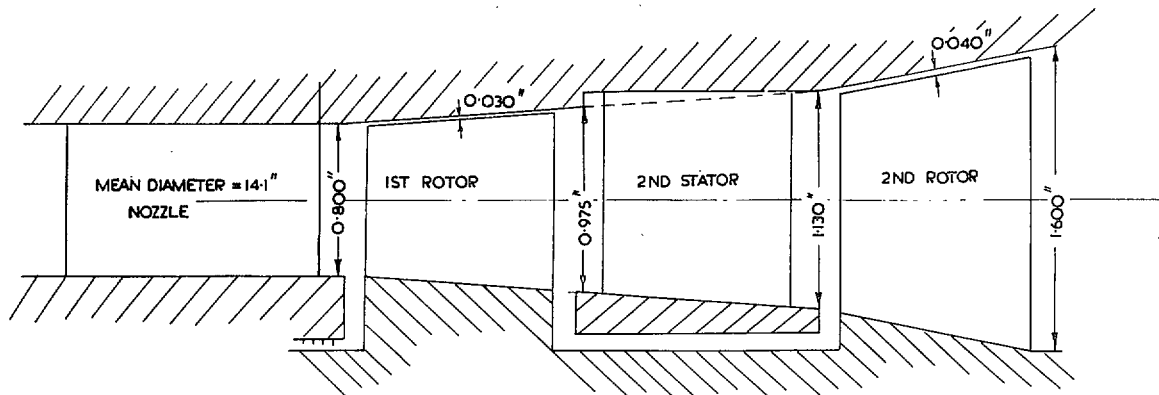


FIG. 3. Turbine annulus dimensions.

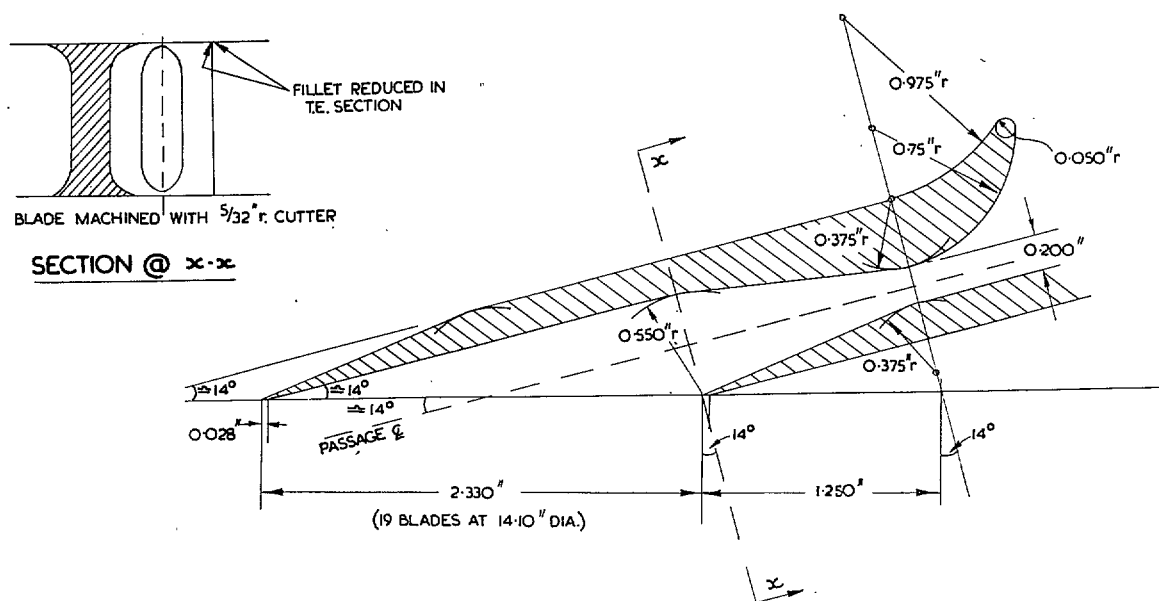
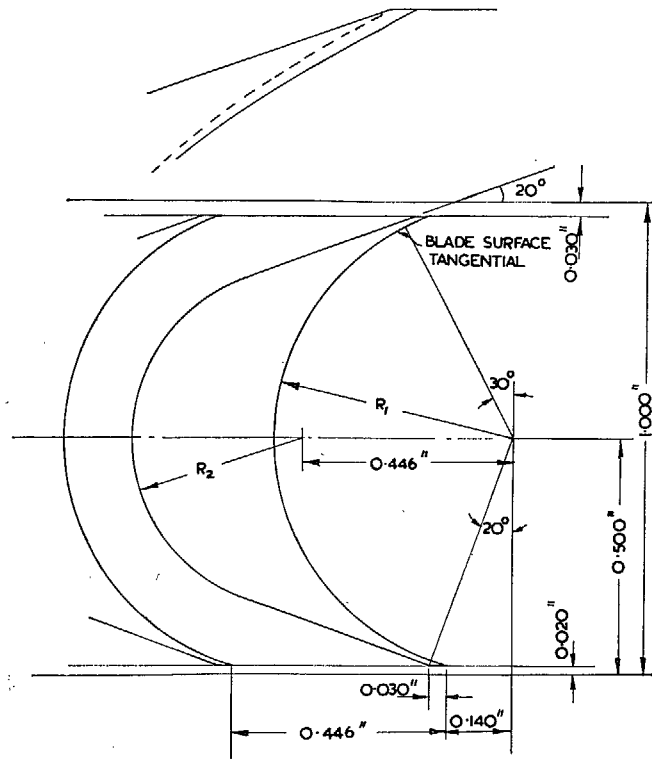
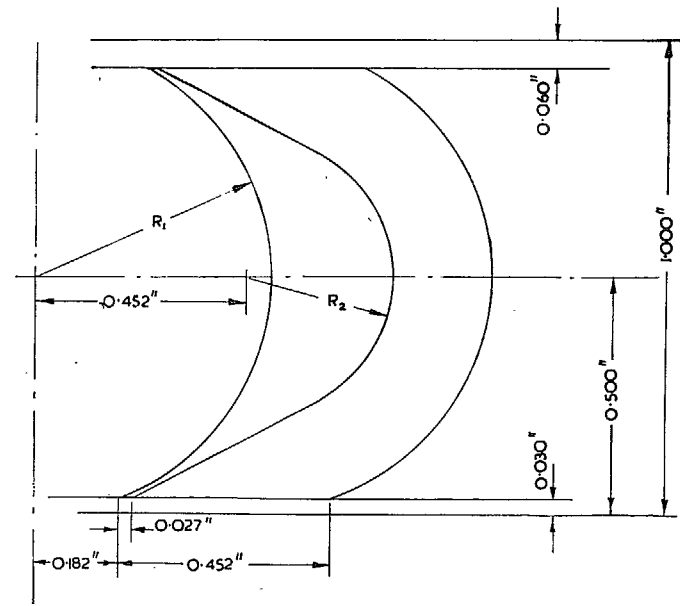


FIG. 4. First-stage nozzle profile at mean diameter. (Mean diameter = 14.1 in.)



NO. OF BLADES = 99
 $R_1 = 0.500''$
 $R_2 = 0.358''$

FIG. 5. First-stage rotor blade profile.



NO. OF BLADES = 98
 $R_1 = 0.500''$
 $R_2 = 0.300''$

FIG. 6. Second-stage stator blade profile.

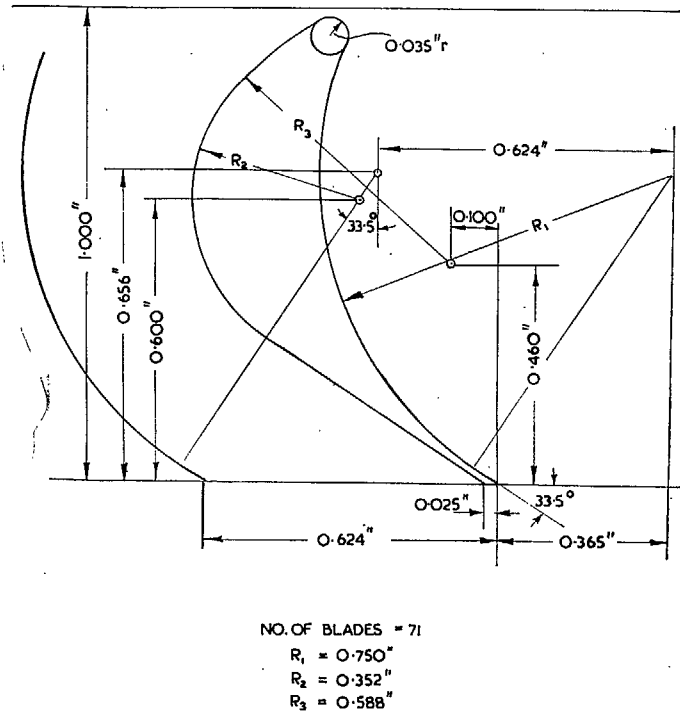


FIG. 7. Second-stage rotor blade profile.

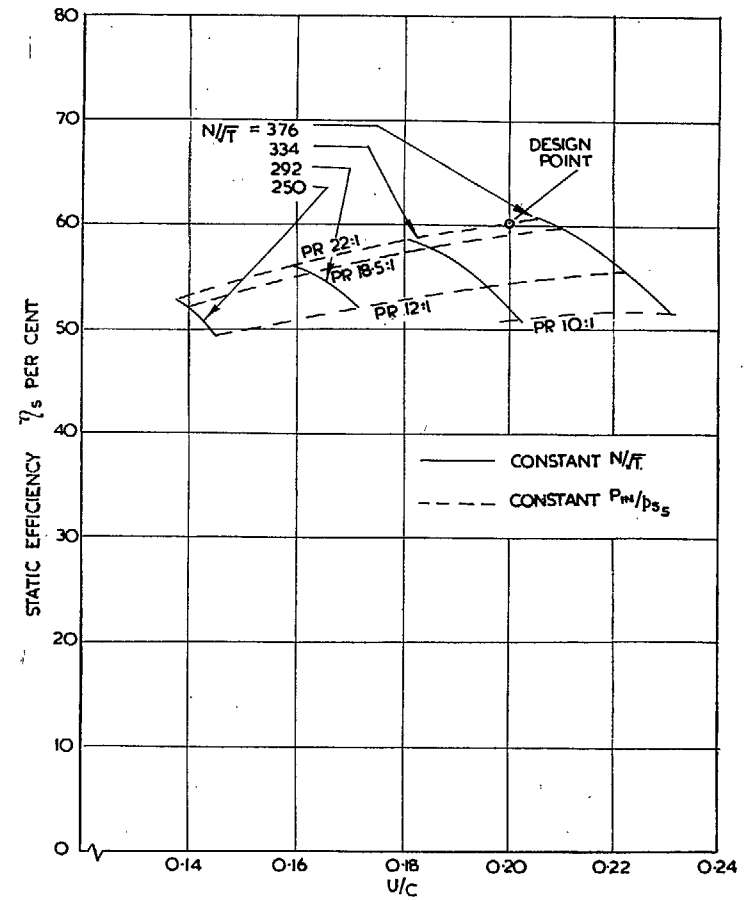


FIG. 8. Static efficiency vs. u/c for two-stage build.

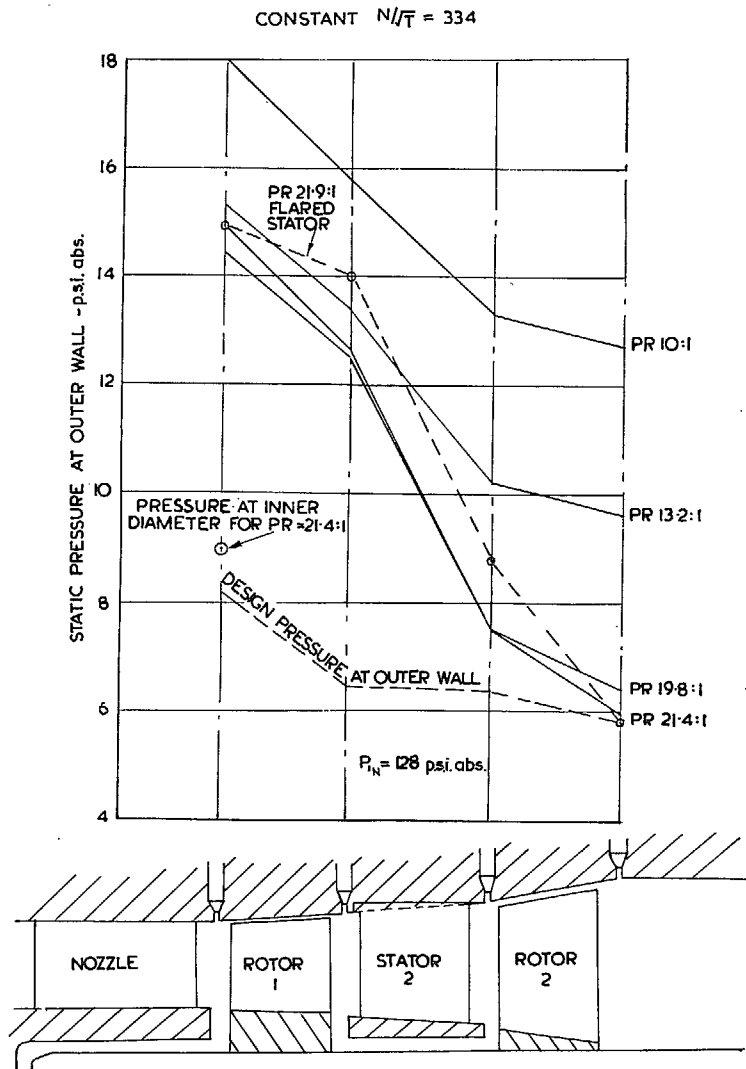


FIG. 9. Pressure distribution for two-stage original blading with unflared second stator.

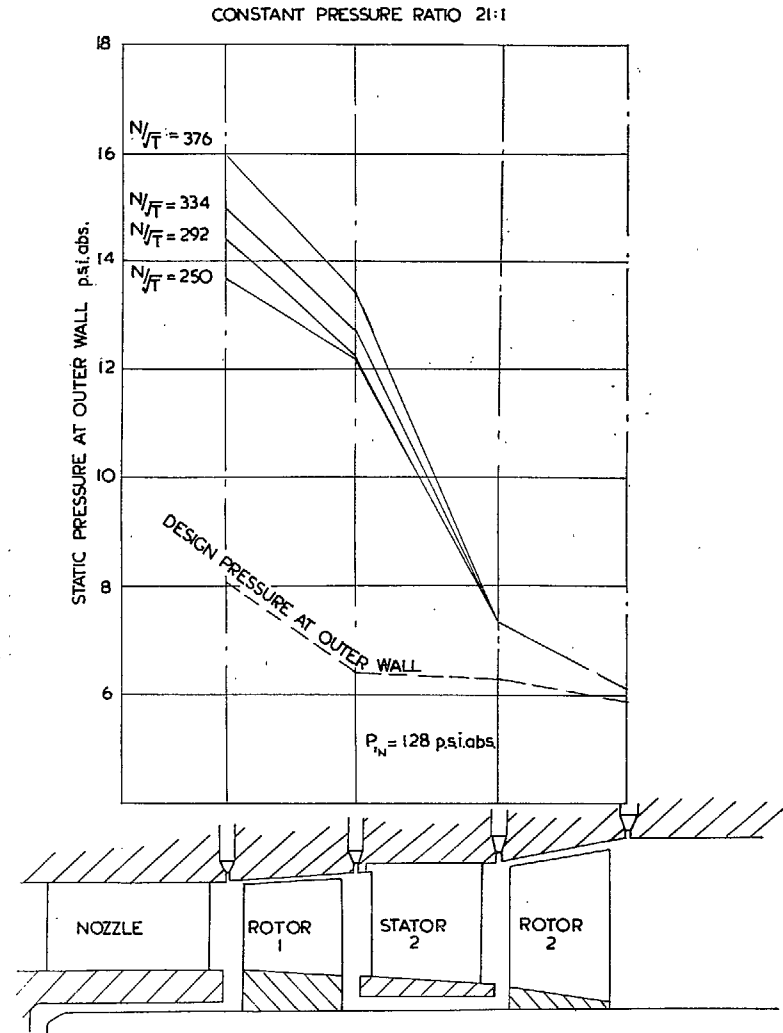


FIG. 10. Pressure distribution for two-stage original blading with unflared second stator.

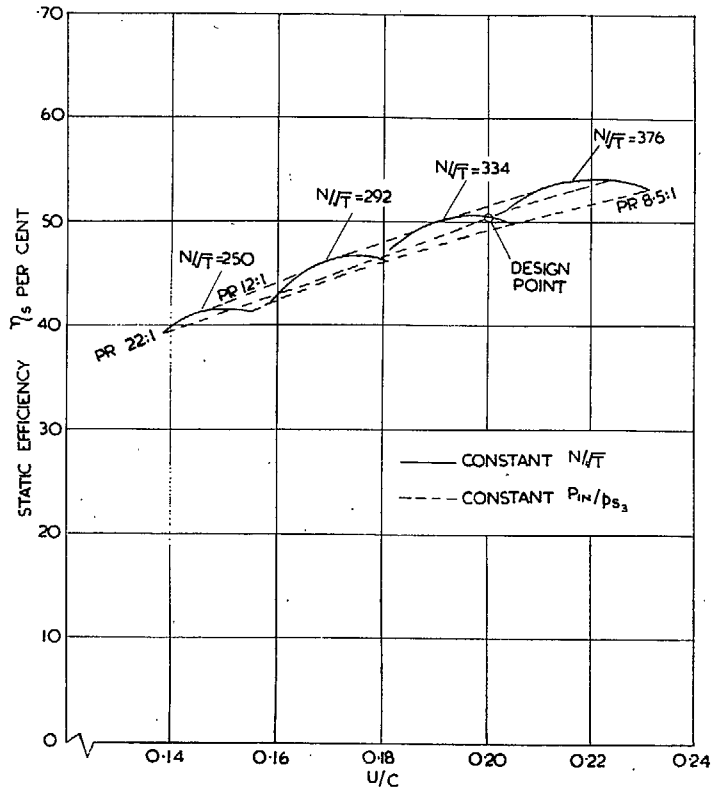
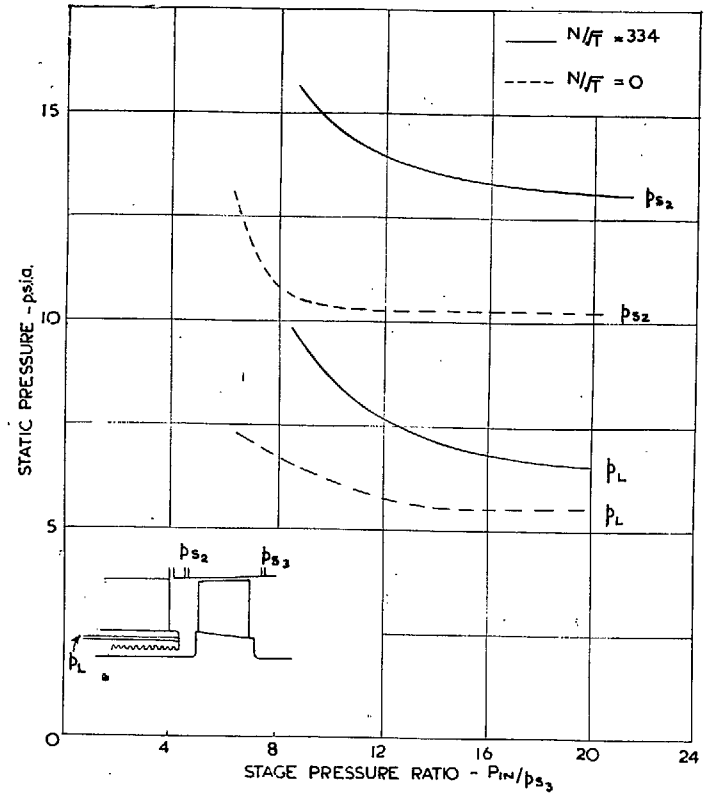


FIG. 11. Static efficiency vs. u/c for single-stage build.



p_{s2} = STATIC PRESSURE NOZZLE EXIT OUTER WALL
 p_L = STATIC PRESSURE NOZZLE EXIT INNER WALL
 PRESSURES CORRECTED TO AN INLET TOTAL PRESSURE (P_{1N}) OF 128 psia.

FIG. 12. Single-stage build, test 1. Nozzle exit pressure vs. stage pressure ratio.

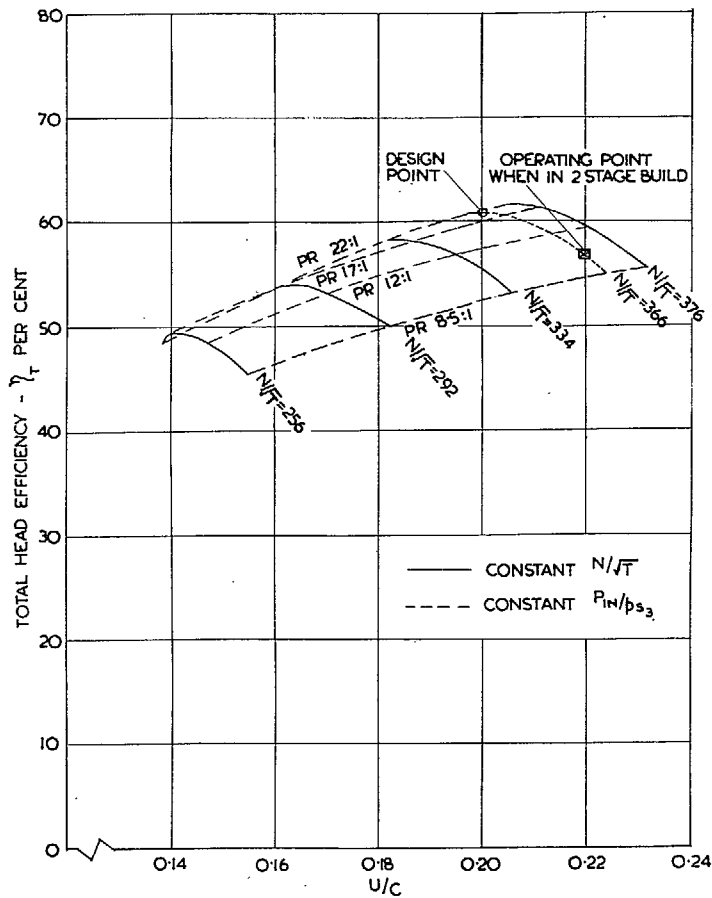
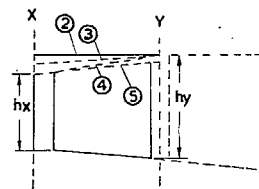
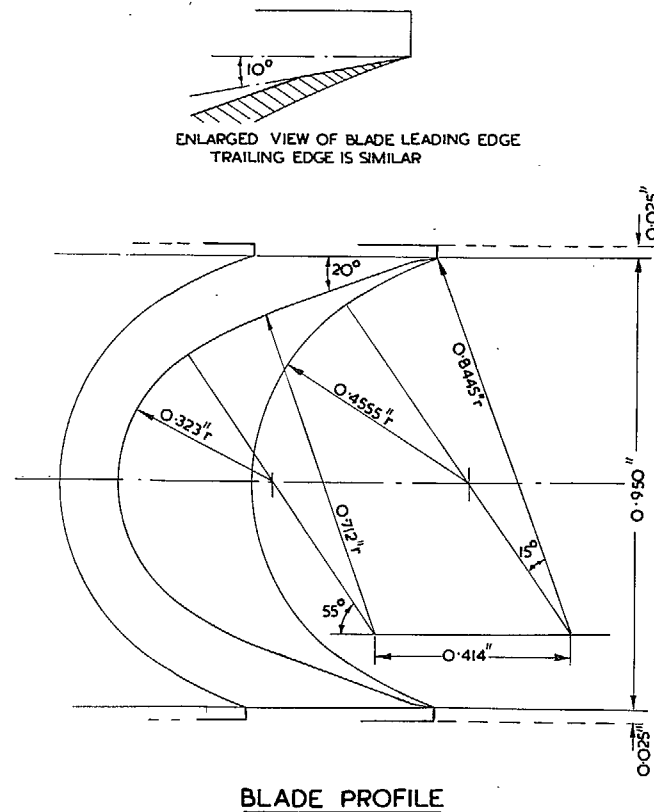


FIG. 13. Total head efficiency vs. u/c for single-stage build.



BUILD No.	2	3	4	5
hx	0.965	0.882	0.800	0.800
hy	1.053	1.053	1.053	0.975

FIG. 14. Second design, first-stage turbine rotor blade profile and spanwise configurations.

NOTE: AVERAGE RUNNING TIP CLEARANCE
APPROX. 0.030"

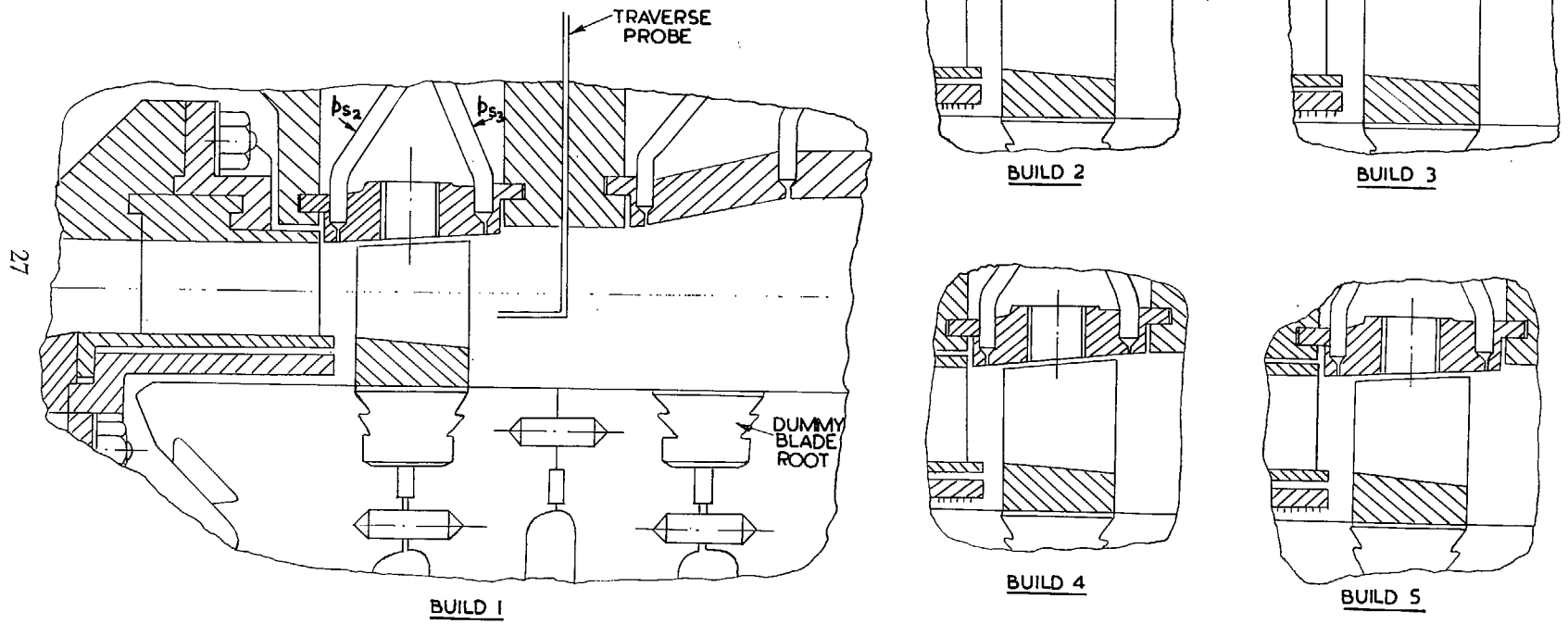


FIG. 15. Turbine arrangements for single-stage testing.

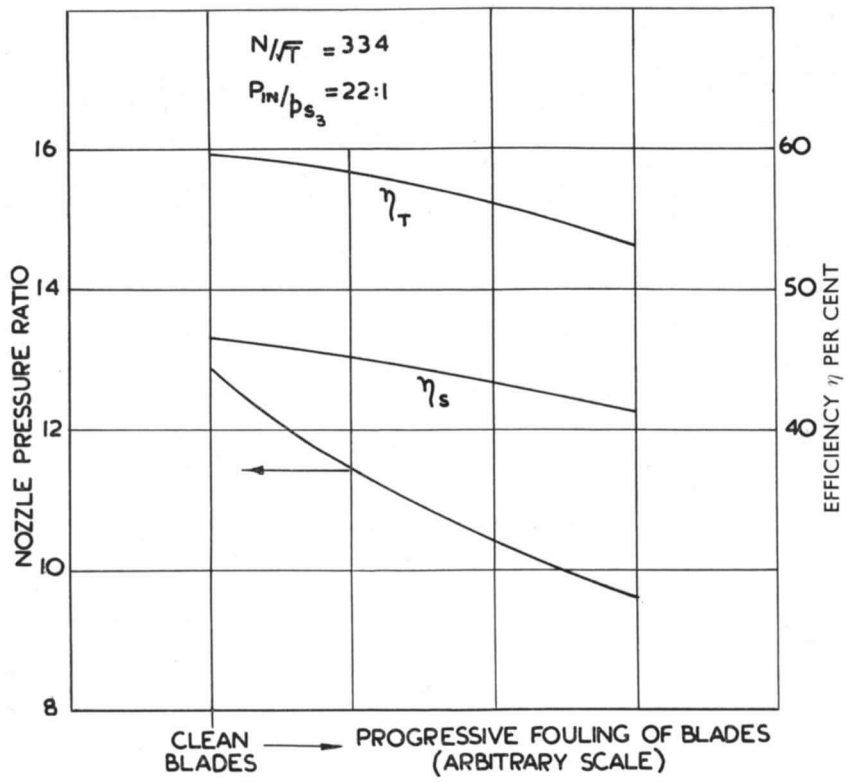


FIG. 16. The effects of blade fouling.

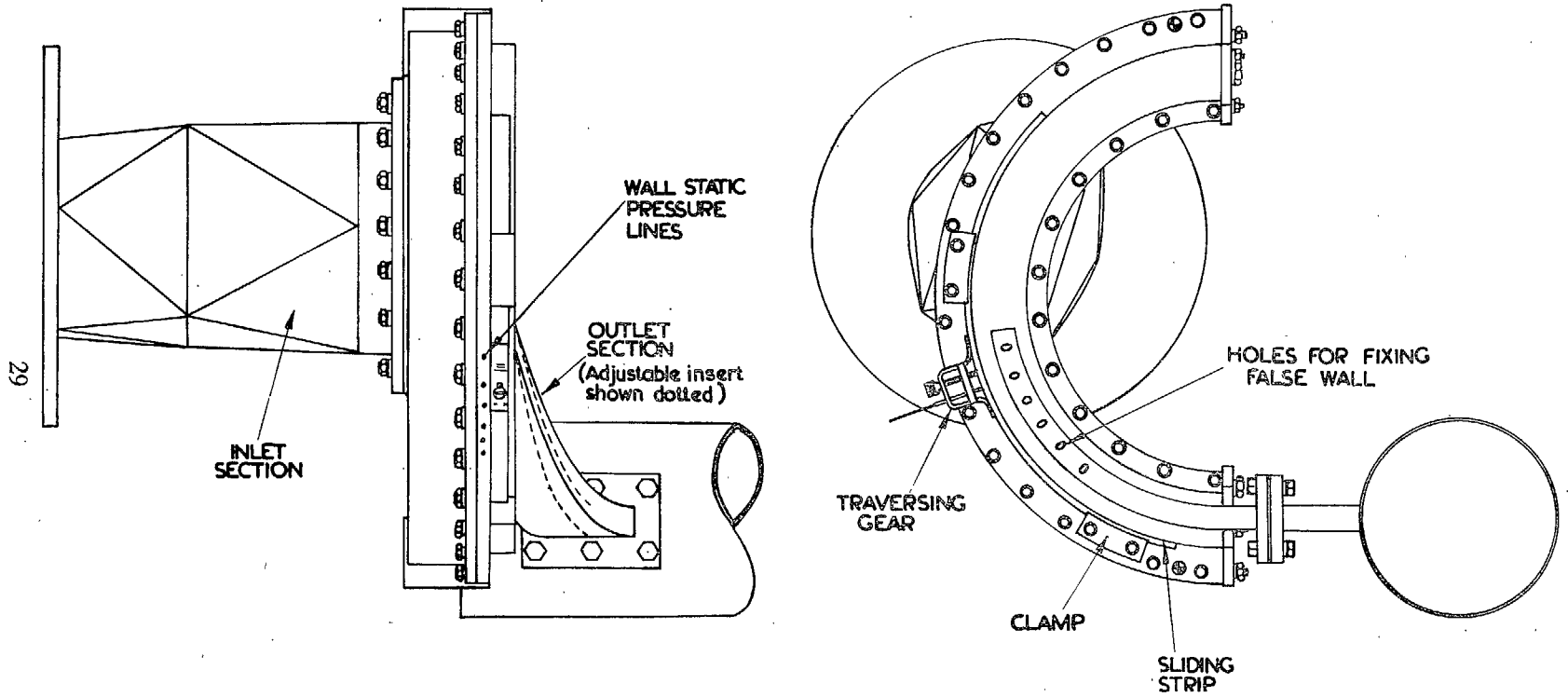
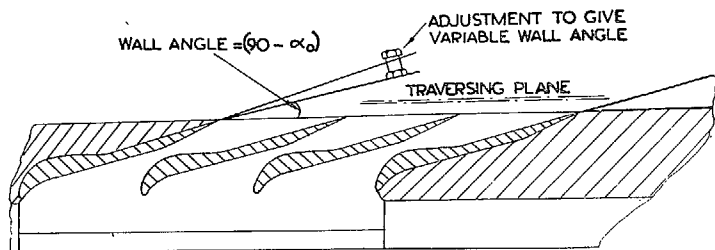
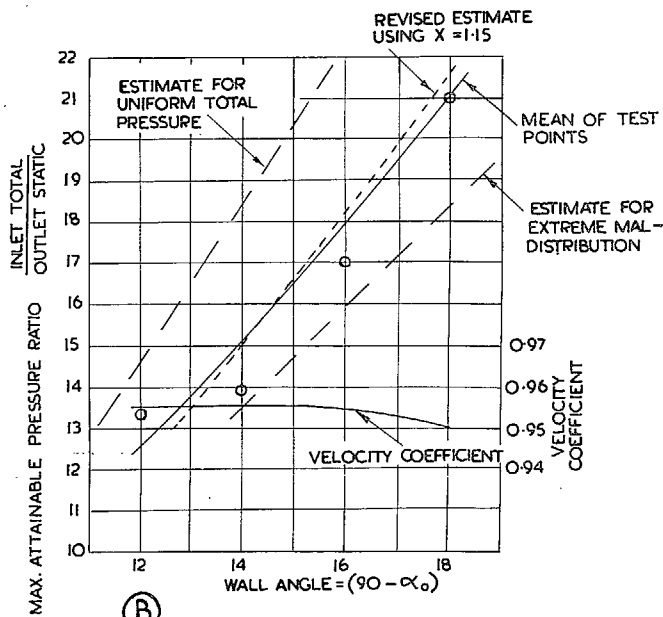


FIG. 17. Three-dimensional nozzle cascade test rig.



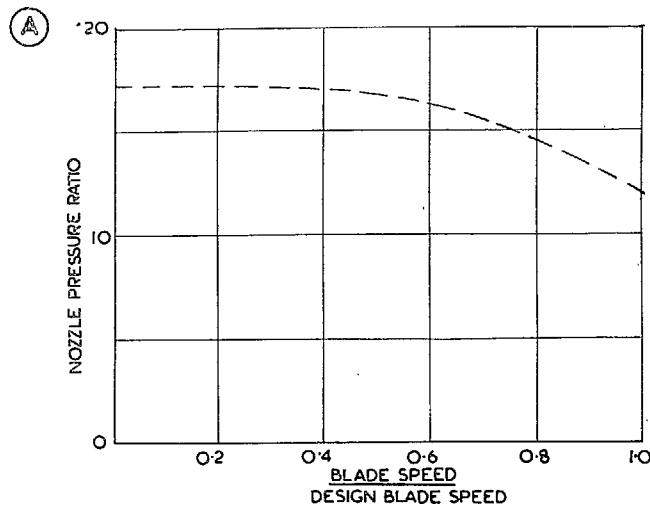
(A)



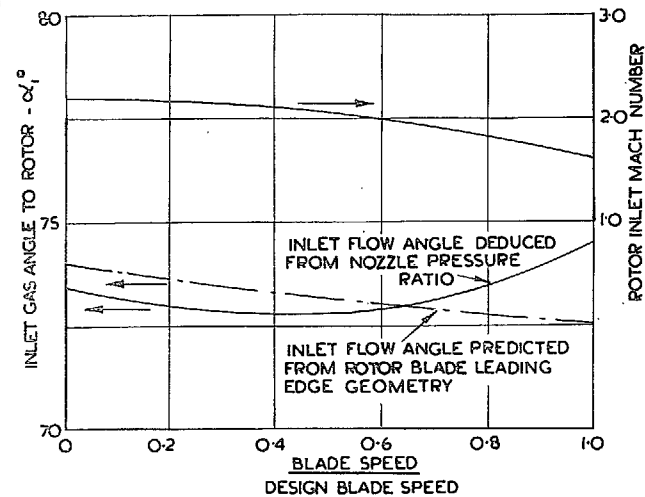
(B)

FIG. 18. Three-dimensional nozzle cascade with variable exit wall angle.

CONSTANT PRESSURE RATIO 22:1



(A)



(B)

FIG. 19. Rotor incidence effect.

Publications of the Aeronautical Research Council

ANNUAL TECHNICAL REPORTS OF THE AERONAUTICAL RESEARCH COUNCIL (BOUND VOLUMES)

- 1941 Aero and Hydrodynamics, Aerofoils, Airscrews, Engines, Flutter, Stability and Control, Structures. 63s. (post 2s. 3d.)
- 1942 Vol. I. Aero and Hydrodynamics, Aerofoils, Airscrews, Engines. 75s. (post 2s. 3d.)
Vol. II. Noise, Parachutes, Stability and Control, Structures, Vibration, Wind Tunnels. 47s. 6d. (post 1s. 9d.)
- 1943 Vol. I. Aerodynamics, Aerofoils, Airscrews. 80s. (post 2s.)
Vol. II. Engines, Flutter, Materials, Parachutes, Performance, Stability and Control, Structures. 90s. (post 2s. 3d.)
- 1944 Vol. I. Aero and Hydrodynamics, Aerofoils, Aircraft, Airscrews, Controls. 84s. (post 2s. 6d.)
Vol. II. Flutter and Vibration, Materials, Miscellaneous, Navigation, Parachutes, Performance, Plates and Panels, Stability, Structures, Test Equipment, Wind Tunnels. 84s. (post 2s. 6d.)
- 1945 Vol. I. Aero and Hydrodynamics, Aerofoils. 130s. (post 3s.)
Vol. II. Aircraft, Airscrews, Controls. 130s. (post 3s.)
Vol. III. Flutter and Vibration, Instruments, Miscellaneous, Parachutes, Plates and Panels, Propulsion. 130s. (post 2s. 9d.)
Vol. IV. Stability, Structures, Wind Tunnels, Wind Tunnel Technique. 130s. (post 2s. 9d.)
- 1946 Vol. I. Accidents, Aerodynamics, Aerofoils and Hydrofoils. 168s. (post 3s. 3d.)
Vol. II. Airscrews, Cabin Cooling, Chemical Hazards, Controls, Flames, Flutter, Helicopters, Instruments and Instrumentation, Interference, Jets, Miscellaneous, Parachutes. 168s. (post 2s. 9d.)
Vol. III. Performance, Propulsion, Seaplanes, Stability, Structures, Wind Tunnels. 168s. (post 3s.)
- 1947 Vol. I. Aerodynamics, Aerofoils, Aircraft. 168s. (post 3s. 3d.)
Vol. II. Airscrews and Rotors, Controls, Flutter, Materials, Miscellaneous, Parachutes, Propulsion, Seaplanes, Stability, Structures, Take-off and Landing. 168s. (post 3s. 3d.)

Special Volumes

- Vol. I. Aero and Hydrodynamics, Aerofoils, Controls, Flutter, Kites, Parachutes, Performance, Propulsion, Stability. 126s. (post 2s. 6d.)
- Vol. II. Aero and Hydrodynamics, Aerofoils, Airscrews, Controls, Flutter, Materials, Miscellaneous, Parachutes, Propulsion, Stability, Structures. 147s. (post 2s. 6d.)
- Vol. III. Aero and Hydrodynamics, Aerofoils, Airscrews, Controls, Flutter, Kites, Miscellaneous, Parachutes, Propulsion, Seaplanes, Stability, Structures, Test Equipment. 189s. (post 3s. 3d.)

Reviews of the Aeronautical Research Council

1939-48 3s. (post 5d.)

1949-54 5s. (post 5d.)

Index to all Reports and Memoranda published in the Annual Technical Reports

1909-1947

R. & M. 2600 6s. (post 2d.)

Indexes to the Reports and Memoranda of the Aeronautical Research Council

Between Nos. 2351-2449

R. & M. No. 2450 2s. (post 2d.)

Between Nos. 2451-2549

R. & M. No. 2550 2s. 6d. (post 2d.)

Between Nos. 2551-2649

R. & M. No. 2650 2s. 6d. (post 2d.)

Between Nos. 2651-2749

R. & M. No. 2750 2s. 6d. (post 2d.)

Between Nos. 2751-2849

R. & M. No. 2850 2s. 6d. (post 2d.)

Between Nos. 2851-2949

R. & M. No. 2950 3s. (post 2d.)

Between Nos. 2951-3049

R. & M. No. 3050 3s. 6d. (post 2d.)

HER MAJESTY'S STATIONERY OFFICE

from the addresses overleaf

© *Crown copyright 1962*

Printed and published by
HER MAJESTY'S STATIONERY OFFICE

To be purchased from
York House, Kingsway, London W.C.2
423 Oxford Street, London W.1
13A Castle Street, Edinburgh 2
109 St. Mary Street, Cardiff
39 King Street, Manchester 2
50 Fairfax Street, Bristol 1
35 Smallbrook, Ringway, Birmingham 5
80 Chichester Street, Belfast 1
or through any bookseller

Printed in England